Ind. J. Pharm. Edu. Res., 2023; 57(3s):s555-s563.
https://www.ijper.org

Original Article

Preparation and Optimization of Microwave-Assisted Ball-Milled Olmesartan Medoxomil with Chitosan Using Full 3^2 Factorial Design

Atul Shivaji Gurav[1, 2,*], Ajit Shankarrao Kulkarni[3]

[1]Department of Pharmaceutics, Gourishankar Education Society's Satara College of Pharmacy, Satara, Maharashtra, INDIA.
[2]Department of Pharmaceutics, Late Adv. Dadasaheb Chavan Memorial Institute of Pharmacy, Malwadi, Masur, Karad, Satara, Maharashtra, INDIA.
[3]Department of Pharmaceutics, Gourishankar Institute of Pharmaceutical Education and Research, Limb, Satara, Maharashtra, INDIA.

ABSTRACT

Introduction: The anti-hypertensive drug Olmesartan Medoxomil (OLM), a BCS II drug, works by inhibiting the action of angiotensin II on AT1 receptors. **Objectives:** The purpose of the study was to enhance solubility and stability by altering crystalline form, which reduces cost and dose burden of the pharmaceutical industry. In the current study, OLM formulation was prepared by using a full 3 level 2 factorial design with chitosan and neusiline as independent factors. **Materials and Methods:** Chitosan, a hydrophilic and stabilizing polymer, was used to enhance solubility and stability with the help of neusiline as a surfactant. Formulation was prepare using microwave-assisted ball milled technology. **Results and Discussion:** In comparison to the pure drug, phase solubility study shows the ternary mixture's saturation solubility was around 12 times higher. Physical interaction between polymer and OLM was confirmed from the FTIR study, DSC graph, SEM surface morphological study and NMR study. The drug's altered crystalline form has been confirmed by XRD, which could alter its solubility and rate of dissolution. The optimized batch obtained from factorial design was used for electrically operated ball milling. This demonstrated a notable improvement in the solubility, stability, and dissolving rate. **Conclusion:** As a result, using chitosan with a microwave assisted ball milling process can be a novel breakthrough in enhancing the bioavailability of any BSC II medicines.

Keywords: Microwave-assisted milling technology, Chitosan, Olmesartan, Neusiline, Factorial Design.

Correspondence:
Mr. Atul Shivaji Gurav
Assistant Professor, Department of Pharmaceutics, Late Adv. Dadasaheb Chavan Memorial Institute of Pharmacy, Malwadi, Masur, Karad, Satara, Maharashtra, INDIA.
Email: atulgurav800@gmail.com

Received: 22-11-2022;
Revised: 23-01-2023;
Accepted: 30-03-2023.

INTRODUCTION

Olmesartan Medoxomil is a prodrug consisting esterified parent compound of olmesartan, 5-(2-hydroxypropan-2-yl)-2-propyl-3-[[4-[2-(2*H*-tetrazol-5-yl) phenyl] phenyl] methyl] imidazole -4- carboxylic acid), with a (5-methyl-2-oxo-1,3-dioxol-4-yl) methyl (Medoxomil).[1] It is the modified imidazole ring-based compound developed by Sankyo chemists.[2] Medoxomil linkage gets deesterified rapidly and converted to active moiety by aryl esterase enzyme found in both intestine and plasma.[3]

In RAS, Angiotensinogen (synthesized by the liver) is converted into Angiotensin 1 (AT1) and then (AT2) by ACE or non-ACE enzymes. OLM antagonizes the action of AT2 on angiotensin receptor 1 (ATR-1) which is predominantly responsible for hypertension and blood vessel contraction.[4] OLM is present in crystalline nature and thus belongs to BCS class 2 having very low solubility in physiological PH. Due to this, its bioavailability is comparatively low, 4.5% to 28.6%.[5-7] Many researchers work on bioavailability improvement using different pharmaceutical approaches like micronization,[8] Nanonization,[8,9] polymeric interaction,[10] spray drying,[11] freeze drying,[12] solid dispersion technologies,[13] etc.

Microwave-assisted milling Technology is a novel technique to stabilize the milled product of crystalline solids by top-down media milling technique.[14] Crystalline particles may be affected by microwave radiation due to changes in internal thermal energy.[15] Therefore, it may have an impact on the glassy or rubbery condition of pharmaceutical crystals, which may result from the interaction of energy with the intermolecular force of attraction.[16]

It was shown that crystalline molecules interact physically with chitosan, a derived polysaccharide produced naturally from the outer skeleton of seawater crustaceans, to increase its stability and

DOI: 10.5530/ijper.57.3s.64

bioavailability. Chemically, chitosan is (1, 4)-2-Amino-2-deoxy-beta-D-glucan obtained from chitin, n- acetyl glucosamine, by deacetylation.[17]

Neusilin US2, $Al_2O_3 \cdot MgO \cdot 1,7SiO_2 \cdot xH_2O$, is a neutral-pH, synthetic, amorphous form of Magnesium Aluminometasilicate that can be employed in the direct compression and wet granulation of solid dosage forms. It can modify powder and dosage form characteristics to improve bioavailability.

Current research focuses on the impact of microwave radiation with the help of ball milling on crystalline materials' physical, chemical, and pharmaceutical characteristics of OLM as an active pharmaceutical ingredient.

MATERIALS AND METHODS

OLM and NS2 were gifted by CTX life sciences limited and Lupin Research Park, Pune for the present investigation. 93% deacetylation of CH was purchased from Loba chemical, India. All the substances/ ingredients and solvents of analytical grade were used without any further purification.

Phase solubility study

By the procedure outlined by Higuchi and Connors, the phase solubility tests of OLM were carried out in distilled water. In 10 mL of distilled water, excess OLM was introduced in the presence and absence of various CH concentrations, either with or without NS2. A mechanical shaker (Bio Technics India) was used to stir a solubility tube holding binary and ternary suspension for 48 hr at room temperature. Whatman filter paper no. 41 was used to filter the suspension equilibrium, and the filtrate was then examined by UV spectroscopy with the appropriate dilutions. The calibration curve of the OLM was used to construct the straight line equation, $y = 0.0118x + 0.0084$, using the maximum wavelength of 255 nm.[18]

Determination of stoichiometric constant

It was determined using different ratios of the molar concentrations of OLM and CH. A suspension was created by combining an increasing OLM molar concentration with a reducing CH molar concentration. Then, this binary combination was kept on a mechanical shaker for 48 hr. It was then filtered using Whatman Filter Paper No. 41 before being examined using a UV-spectrometer at 255 nm.[18]

Experimental work

Preparation of ternary complex

Selection of factors

From preliminary data of the stoichiometric study and phase solubility study, the percentage of CH and % NS2 were chosen as two independent variables X1 and X2 with three levels. A 3^2 level full-factorial design with Design Expert version 12 was used to formulate and optimize ternary complexes. As indicated in Table 1, this results in a total of 9 experimental batches for evaluation of the dependable responses Y1; saturation solubility, and Y2; % drug release. These variables were examined to achieve an optimized batch with the highest response.[19,20]

Formulation of ternary complexes

Microwave Assisted Grinding Technology (MAGT)

Crystal particles were prepared using a microwave-assisted grinding technique.

A number of ingredients were weighed and ground for roughly 20 min in a mortar and pestle. This mixture was made into a thick slurry by adding a sufficient quantity of distilled water. The slurry was applied to the inside of the beaker and placed inside a microwave (Panasonic microwave oven, 230V, 50 Hz, 1250W) set at 800 W power for 3 min. It was taken out, well mixed, and then subjected to another 3 min of microwave radiation treatment. In a desiccator, the dried ternary complex was cooled and collected. The quantity of X1 and X2 was optimized using dependable variables.[21]

This optimized batch was chosen for size reduction using an electrically powered ball mill (Shreeji Chemicals, Kandivali, Mumbai) at 100 rpm for 48 hr. Four types of ball were used with varying radius for impact and attrition.

Saturation solubility studies

According to the Higuchi and Connors approach, saturation solubility was investigated in distilled water and a dissolution media. Excess OLM and prepared particles were added to solubility tubes containing 10 mL of solvent, and the tubes were mechanically shaken for 48 hr at room temperature with a speed of 100 rpm. After reaching equilibrium, the solution was filtered and, if necessary, diluted. Using UV-spectroscopy at 255 nm, the saturation solubility of the filtrate was examined.[22]

Fourier Transformation-Infrared Spectroscopy (FTIR)

Using FTIR (BRUKER - ECO - ATR - ALPHA, Germany) spectroscopy, functional group and bond vibrational frequencies of pure OLM, CH, and NS2 were observed separately. This procedure was applied for physical mixtures and formulated crystal particles using various techniques. The samples were placed directly on the pan and subjected to 24 scans in the 600 to 4000 cm^{-1} spectral range.[23]

Percentage drug content studies

Accurately weighed crystal particles, equivalent to the dose, from all drug formulation batches, were added in solubility tubes with 10 mL of DMSO. At room temperature and a speed of 100 rpm, this was swirled mechanically for 24 hr. After reaching equilibrium, it was filtered through Whatman filter paper No. 41

and subjected to the necessary dilution UV-spectroscopy analysis utilizing Shimadzu UV-spectroscopy at 256 nm wavelength. The following formula was used to determine the percentage of drugs present.

$$\% \text{ drug content} = \frac{\text{actual drug content in methanol}}{\text{theoretical equivalent drug taken}} \text{ X } 100$$

Differential Scanning Calorimetry (DSC)

Pure OLM, CH, NS2, physical mixture and formulated crystal particles were thermal analyzed using a DSC analyzer (TA Instruments, SDT Q600 USA). Over the temperature range of 40-260°C, a sample (5 mg) was heated in a nitrogen environment at a heating rate of 20°C/min.[23,24]

X-ray Powder Diffractometry (XRPD)

The XRPD patterns of all systems were recorded by using an X-ray diffractometer (BRUKER – D2 PHA-SER, Germany) with tube anode Cu, over the interval 10–90°/2 hr. The operational data were as lows: Generator tension (voltage) 30 kV, Generator current 10 mA.[23,24]

Nuclear Magnetic Resonance (NMR)

The interaction between the drug and excipient is revealed by the peak for protons in NMR spectrum analysis. It was recorded using a spectral window of about 10,000 Hz at 300 MHz (Bruker, Germany). TMS was used as an internal standard, and samples were dissolved in DMSO as a solvent.[25,26]

Dissolution study

The dissolution study was carried out using a type 2 dissolution apparatus in 900 mL of pH 6.8 phosphate buffer (LABINDIA Dissolution test apparatus, DS 8000). The temperature was kept constant at 37 ± 0.5°C and 50 rpm, respectively. 5 mL of the aliquot was withdrawn and replaced with a fresh buffer after a predetermined period of the time. If necessary, dilute the aliquot and examine UV-spectroscopy for the proportion of drug release at an absorbing wavelength of 255 nm.[27,28]

Stability study

A stability study was carried out in a stability chamber (REMI SC 16S) kept at 40°C and 75% relative humidity. It was carried out over 90 days, with samples taken at the 0, 15, 30, 60, and 90-day marks. Samples were analyzed using UV-spectroscopy and DMSO as the solvent solution to determine the percentage drug concentration.[27]

RESULTS

Phase solubility study

The saturation solubility of OLM in distilled water was found to be 29.2 µg/mL, which was enhanced in a binary mixture of CH and NS2 by about 4.2 and 7.7 times respectively. But as per Figure 1A, enhancement was more than 12 times in a ternary mixture of OLM with CH and NS2.

In formulations containing CH as compared to those without CH, saturation solubility was increased by an increase in NS2 concentration. Variable NS2 and CH concentrations, as seen in Figure 1B and C, also supported this.[18]

Stoichiometric constant determination

It was calculated by plotting a graph of the molar ratio of the drug to CH (r) versus ΔA*r in Figure 1D from the data given below in the Table 2.

FTIR

Chemical interaction between drug and excipients was studied from data obtained from FTIR shown in Figure 2 (1). This shows changes in peak values if presence of any interactions.

DSC

DSC studied in the region of 100°C to 240°C. This study confirms the interaction and any physical change due to the absorption of heat at the point of melting from Figure 2 (2). All peaks showed endothermic peaks in the region of 170°C to 190°C with varying enthalpic areas.

XRD

The maximum peak intensity of OLM in XRD analysis was found to be at 2Θ values of 21.56498 and 16.3394 which in Table 3 and confirms the crystalline nature. Maximum peak intensities of microwave treated without ball milled and with ball milled as shown in the Figure 2 (3).

The surface morphological study for OLM and O_9 batch was depicted in Figure 3. It showed irregularities in particle surface in O_9 due to the interaction of CH in presence of microwave treatment.

Table 1: Factorial batches.

Batch	A: CH (%)	B: NS2 (%)
O_1	5	5
O_2	10	5
O_3	15	5
O_4	5	10
O_5	10	10
O_6	15	10
O_7	5	15
O_8	10	15
O_9	15	15

Table 2: Stoichiometric constant determination.

OLM (mM)	CH (mM)	Total	Abs	r	ΔA	ΔA*r
1	0	1	0.144	1.00	0.03	0.030
0.8	0.2	1	0.18	0.80	0.036	0.029
0.6	0.4	1	0.247	0.60	0.2	0.120
0.4	0.6	1	0.292	0.40	0.245	0.098
0.2	0.8	1	0.234	0.20	0.187	0.037

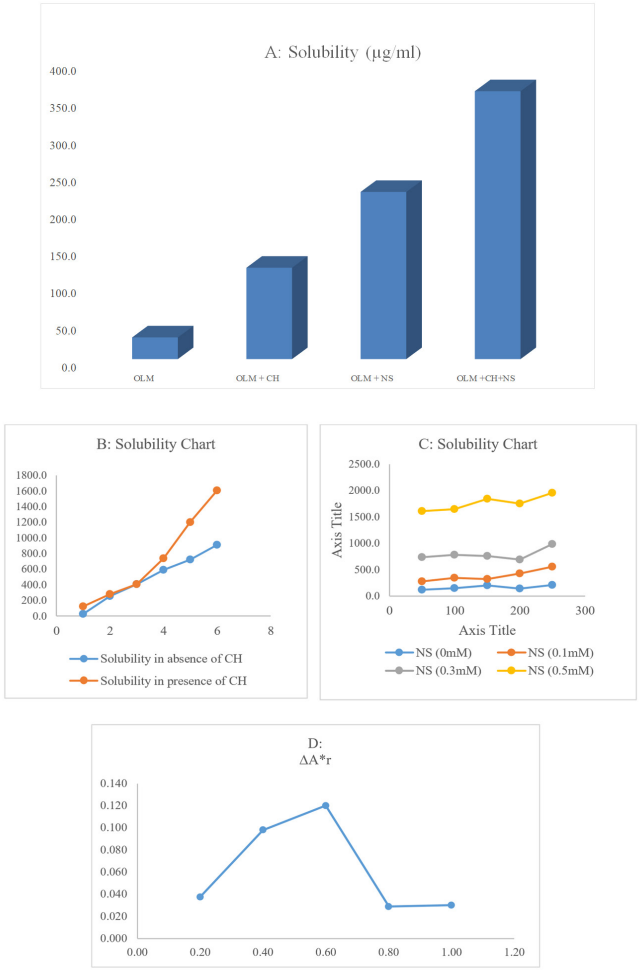

Figure 1: A: Phase solubility study of OLM with binary and ternary physical complex; B: Solubility study of OLM with or without CH; C: Solubility study of OLM with varying amounts of NS2; D: A graph of the molar ratio of drug to CH (r) versus ΔA*r.

NMR

Sharp peaks for chemically and magnetically different protons and their splitting due to neighbouring protons as shown in Figure 2 (4) for OLM and formulation batch. All peaks were present within 18 ppm from a reference point.

Saturation solubility study

The saturation solubility of all formulation batches with OLM is in the Figure 4 (1) given below.

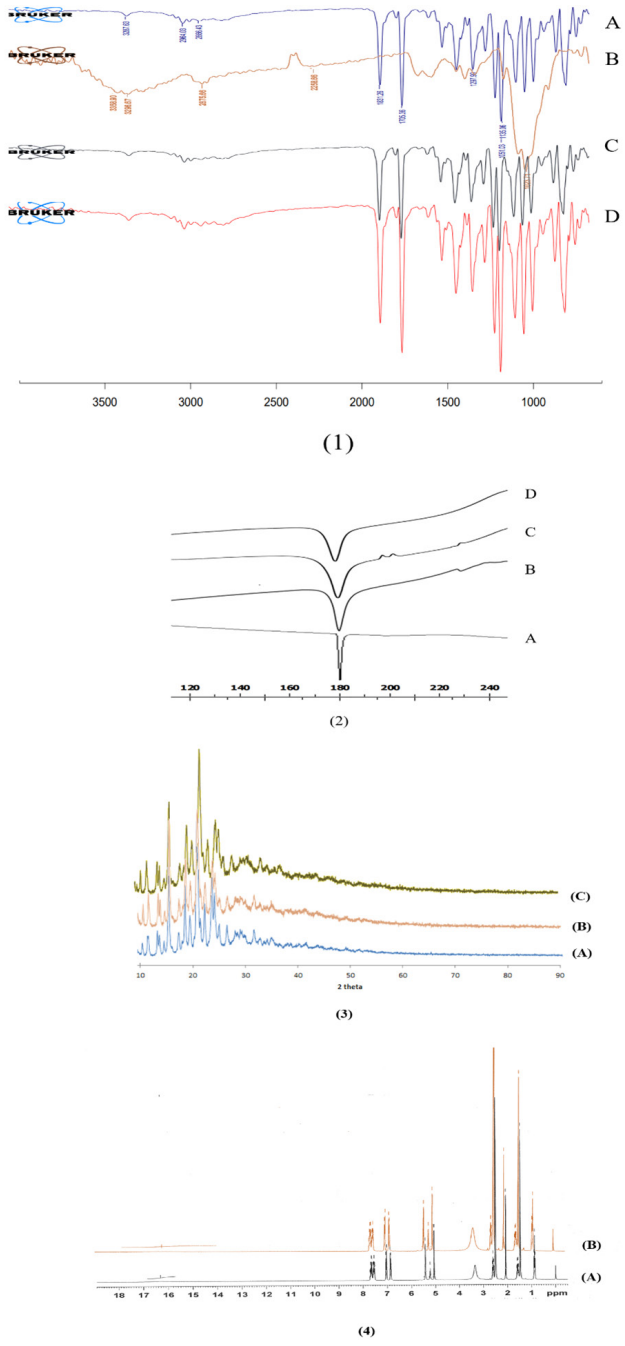

Figure 2: (1): FTIR peaks of A- OLM; B- CH; C- OLM Form and D- OLM ball milled; (2): DSC graphs of A: OLM; B: OLM with microwave; C: O_9 with microwave; D: O_9 ball milled; (3): XRD study of A: OLM; B: formulation without ball milling; C: formulation with ball milling; (4): NMR spectrum peaks of A: OLM; B: Formulation O_9.

Table 3: Theta values of various batches.

Batch	2 Theta value	
	21.5649	16.3394
OLM	3669	2577
Oph	1816	1745
O_9	1687	1401

Oph: OLM physical mixture, O_9: OLM formulation batch 9.

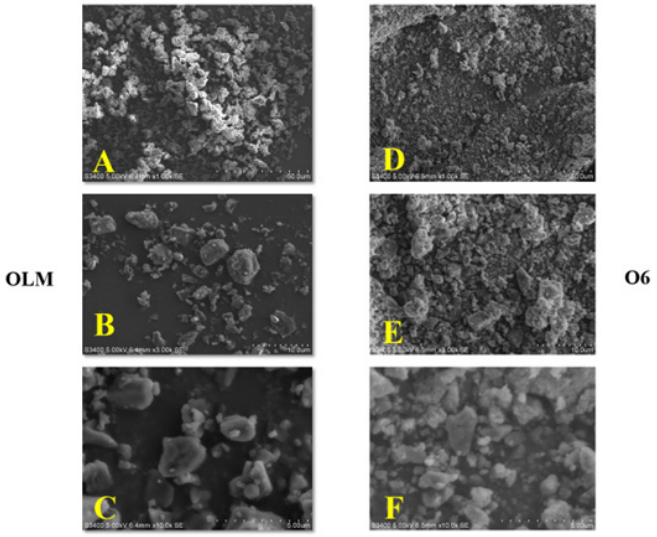

Figure 3: SEM image of OLM (A, B and C with magnification to 50 µm, 10 µm and 5 µm) and O_9 (D, E and F with magnification to 50 µm, 10 µm and 5 µm).

It is one of the variable factors for the optimization of formulation batches by using design expert software. A quadratic model was selected from the coefficient of regression for the optimization of saturation solubility. The contour and 3D plot were estimated from software depicted in Figure 4 (2). The model was significant from the ANOVA study which showed *F*- value of 51.73 with a *p*-value of 0.0041. The predicted R^2 of 0.8778 was in reasonable agreement with the adjusted R^2 of 0.9694; i.e., the difference is less than 0.2 which indicates better adequate precision. Perturbation plot shows curve line in Figure 4 (3) with two factors indicates interaction in saturation solubility of OLM. In this case, A, B, B^2 are significant model terms having *p*-value < 0.0500, where A and B are varying percentages of CH and NS2 respectively. The final Equation in terms of coded factors for saturated solubility shows positive and synergistic effect of A, B, AB, A^2 and B^2. This equation is given as,

$$\text{Saturation Solubility} = 915.04 + 301.63\ A + 241.45\ B + 18.3\ AB + 44.73\ A^2 + 142.28\ B^2$$

Dissolution study

The percentage cumulative drug release from OLM and batches was calculated and plotted as shown in the dissolution profile Figure 5 (1). % CDR for OLM was found to be 22.17%. All formulated batches were releasing a maximum drug than OLM

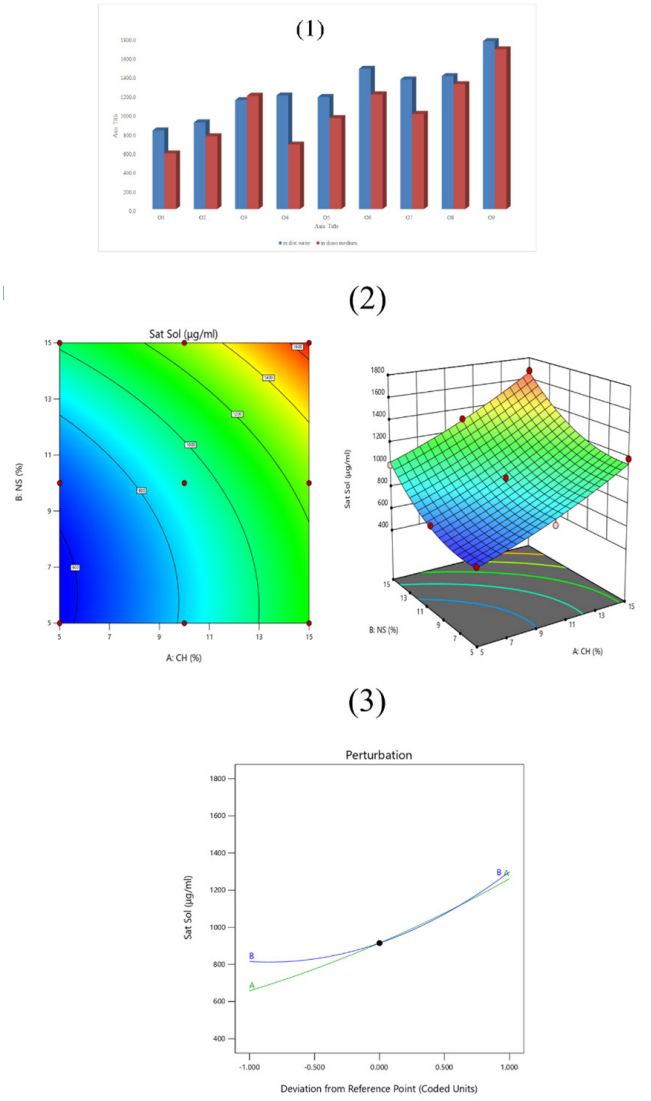

Figure 4: (1): Saturation solubility study of all formulated batches; (2): Contour and 3D plot between factors and saturation solubility; (3): Perturbation plot for saturation solubility study.

with batch O9 showed a maximum % CDR as an optimized batch for comparison with ball milled formulation. Ball milled batch showed a slightly maximum % CDR but maximum rate of drug release in the initial time duration Figure 5 (2).

A design expert version 12 tool was used for optimizing the maximum cumulative drug release of all formulated batches. Depending upon coefficient of regression, it was suggested a quadratic model for the effect of variation in % CDR in all batches. ANOVA was significant showing F- value of 60.05 and a p-value of 0.0033 (smaller than 0.005000) with a significant factor of A, B, and A^2. The predicted R^2 of 0.8794 is in reasonable agreement with the adjusted R^2 of 0.9736; i.e., the difference is less than 0.2 which gives adequate precision. Figure 5 (3 and 4) shows the contour and 3D plot of % CDR for two variables. Perturbation plot shows curve line in Figure 5 (5) with two factors indicates interaction in % CDR.

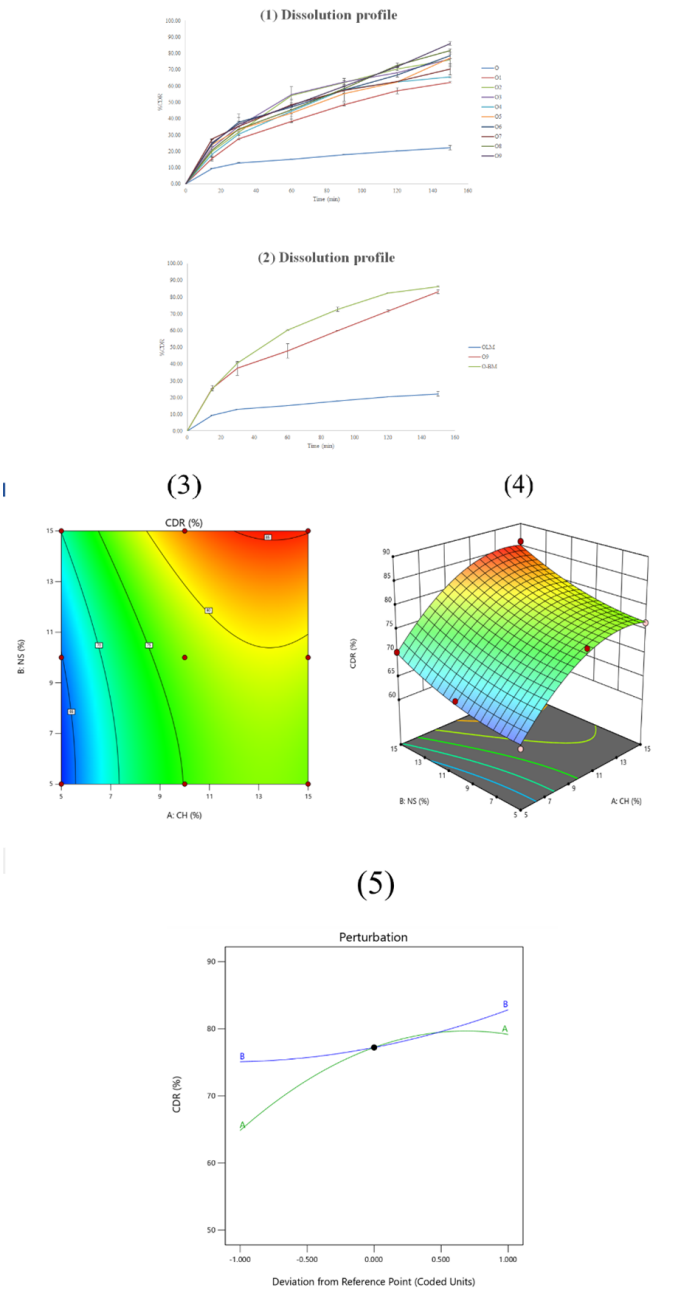

Figure 5: (1): Dissolution profile of all formulated batches with OLM; (2): Comparision of dissolution profile of OLM, O_9 and ball milled O_9; (3): Contour plot between factors and percentage drug release; (4): 3D plot between factors and percentage drug release; (5): Perturbation plot for saturation solubility study.

The coded equation for the quadratic model shows positive and synergistic effect of A, B, AB and B2. Factor A2 shows antagonistic effect due to negative value of coefficient. This equation is given as

$$\%CDR = + 77.2 + 7.16\ A + 3.87\ B + 0.365\ AB - 5.22\ A^2 + 1.74\ B^2$$

Mathematical model for drug release mechanism

Mathematical model was applied to OLM, O_9 and O- BM batches for study of drug release kinetics. Table 4 showed variation in the drug release mechanism with variable coefficients of regression (R^2) value.

Drug Content

Percentage drug content was found in the range of 96.3% to 102% for all formulated batches without treatment of the ball mill. The percentage drug content for ball milled batch was found to be 89.5%.

Stability study

The percentage drug content used for evaluation of stability study for physical mixture without microwave treatment of OLM with CH and NS2, O_9, and O- BM was given in Figure 6 as follows.

DISCUSSION

Phase solubility study

Increased solubility in distilled water suggests that CH and NS2 interact physically and effectively. CH was responsible for the enhancement of wettability and hydrophilic interaction and NS2 was responsible for the reduction of surface tension for OLM. In the presence of ternary complexes with various proportions of CH and NS2, solubility was significantly increased. Increased amounts of CH and NS2 individually as well as in the ternary complex resulted in an increase in solubility as shown in Figure 1A.

Stoichiometric constant determination

As an inorganic surfactant, NS2 has limited use in formulation batches. From the graphical representation of stoichiometry (Figure 1D), the peak of the graph was found to be at about 0.6. Thus, the ratio of OLM to CH was confirmed for 1:0.6.

Table 4: Coefficient of regression value for mathematical model.

Drug release kinetic model	R^2		
	OLM	O_9	O- BM
First Order reaction	0.856	0.9586	0.9937
Zero order reaction	0.8271	0.9406	0.8945
Korsemeyer Peppas	0.9543	0.9551	0.9588
Higuchi	0.9807	0.9939	0.9944
Hixson Crowell	0.8461	0.9752	0.9738

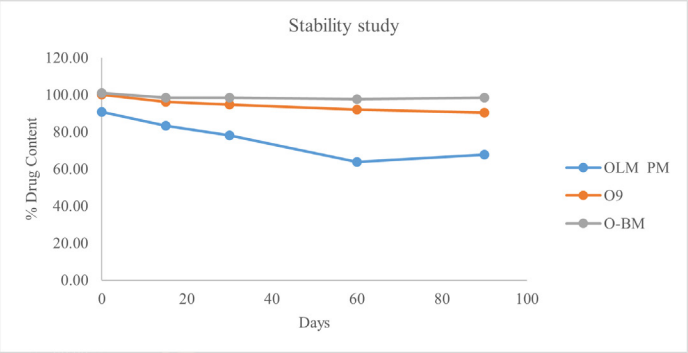

Figure 6: Stability study of OLM, O_9 and ball milled O_9.

FTIR

Olmesartan contains ester (-CO-O), aromatic cyano (-C=N-), and methyl (-C-H) group which showed a sharp stretching peak at 1831.26 cm^{-1}, 1705.36 cm^{-1} and 2866.83 cm^{-1} respectively from Figure 1A. Aromatic secondary amine (N-H) present in chemical structure shows a single peak at 3287.63 cm^{-1}. Alkenyl group (-C=C-) and cyclic alkenes showed a sharp peak at 1603.73 cm^{-1} and 1554.36 cm^{-1} respectively. OLM also consisting an aromatic ester group which showed a stretching peak at 1226.96 cm^{-1}. Figure 1B showed broad peaks at 3358.90, two sharp peaks at 3296.67, a sharp stretching peak at 2875.66, 2258.66 and 1023.71 cm^{-1} which was identified for the alcoholic (OH) group, primary amine (NH_2), SP_3 alkyl group (-CH), C-N bond and etheral C-O respectively. All these peaks are characteristics of hydrophilic CH. As neusiline is an inorganic surfactant, it showed no stretching or bending peaks.

In the formulations shown in Figure 2(1), all of the aforementioned OLM and polymer peaks were visible. The lack of any further peaks and the presence of all functional group peaks indicate that the drug and polymer did not interact chemically.[23] NS2, used in formulation, doesn't show any interaction peak indicating compatibility with OLM.

DSC

OLM showed a sharp endothermic peak at 181.2°C, corresponding to the melting point, with a more endothermic area under the curve. OLM treated with microwave radiations showed an endothermic peak at 180.6°C with somewhat broadening. Formulation with microwave treatment and with ball milling batch showed decreased endothermic peaks at lower values at 178.8°C and 176.2°C respectively. It was concluded from Figure 2(2) that microwave treating and ball milling would be responsible for physical crystallographic changes in OLM. This might be due to the physical interaction of the hydrophilic polymer with crystalline drug and conversion into metastable crystals.[23,24] NS2 might not involve in physical interaction with OLM.

XRD Study

A sharp and most intense peak in the XRD pattern confirms the crystalline nature of OLM from Figure 2(3). Changes in peak intensity at 2Θ to the lower side confirm the interaction and reduction and/or change in crystalline position in formulations. Thus, microwave treatment in the presence of hydrophilic CH affects the crystallinity of the drug by alteration of crystal structure and position. OLM was not completely converted into an amorphous phase due to the presence of intense peaks at particular 2Θ. Thus, OLM changes its crystalline nature to the enhancement of solubility but remains stable in metastable form. This might be due to the presence of CH in the formulation. As NS2 present in amorphous form, it was not affect on crystallinity significantly.

Attrition and impacts in ball milling would change the stability of crystal into metastable form. Hence microwave-treated formulation with ball milling also reduces peak intensity.[23,24]

SEM

From Figure 3, the surface of the drug particle was more regular and granular in nature which might be due to its crystalline form. But after treatment of microwave radiation with simple grinding, it gets converted into a rough and irregular surface indicating a change in the surface energy of OLM. These changes might be due to the brittleness of particles formed by the energy of microwave irradiation between polymer CH and OLM. NS2 reduces surface tension and surface free energy of particle. So, OLM particles in formulations appeared separately with reduced size.

NMR

All protons present in the structure of OLM like aromatic ring proton, SP_2 and SP_3 hybridized, proton attached to hetero atoms, and allylic proton were present in NMR peaks which confirms the structure of OLM. All these peaks from Figure 2(4) were present in the O_9 formulation with a slight downshift in peak values. It might be due to hydrogen bonding with a hetero atom or aromatic ring.[25,26]

Saturation Solubility study

Solubility in distilled water and dissolution medium was enhanced with an increase in the concentration of CH and NS2 (Figure 4(1)). Saturation solubility was maximum in distilled water than dissolution medium, which might be due to the interference of the phosphate group in the solubility of OLM. As per the planar contour graph and the 3D surface graph (Figure 4 (2 and 3) from the design expert tool highest percentage of CH and NS2 was required for maximum saturation solubility.[22] Interaction between two factors were confirmed from perturbation curve (Figure 4 (4)).

Dissolution study

The crystalline form of OLM showed 22.27% cumulative drug release due to low solubility in the dissolution medium. The dissolution pattern showed drug release immediately after contact with a medium which might be due to the low effective intrinsic solubility of OLM crystals. Microwave irradiation in presence of CH affects surface morphological interaction and reduced surface tension using NS2, which is responsible for the enhancement of the dissolution profile of OLM (Figure 5 (1 and 2)). %CDR was enhanced with a concentration of CH and NS2. Thus, batch O_9 showed a maximum %CDR (83.07%) which was about 3.75 times higher than the OLM drug. This was confirmed by the planar contour graph and the 3D surface graph (Figure 5 (3 and 4)). Effect of interaction between two factors on dissolution profile of OLM were confirmed from perturbation curve (Figure 5 (5)).

The ball milling technique helps to increase the effective surface area of the particles. Hence it showed 86.36% CDR with more drug release in the initial phase.[27,28]

According to Table 4, Higuchi model exhibits the highest R^2 value, demonstrating drug release in the dissolving medium without swelling. However, due to a change in crystal structure and molecular internal organisation, the release mechanism in the O_9 batch was improved. Using the Higuchi model, the milling approach demonstrated maximum release kinetics after converting microwave-treated particle into nanocrystals. Initial some burst release was confirmed from R^2 value of first order and zero order model in the ball milled batch.[29]

Drug content

All formulated batches showed maximum drug content. This confirms the physical interaction between CH and NS2. There was the experimental loss of drug in the ball milling method which was not a significant loss.

Stability study

It was confirmed from Figure 6 that OLM irradiated with microwave forms a physical interaction with CH and NS2. A stability study would compare the possible changes due to interaction with moisture at elevated temperatures with OLM, which could change the drug content in batches. It was found from Figure 6 that maximum stability or O-BM with maximum drug content. Thus enhancement of stability would be possible due to the interaction of CH with OLM in the formulation.[27]

CONCLUSION

Due to crystalline form, OLM belongs to BCS II drug having low solubility and hence a low bioavailability. This may enhance the dose and economic burden on pharmaceutical industry. Solubility and stability are the two key factors in bioavailability improvement. The OLM molecule would physically interact with the microwave radiation in the presence of water, resulting in the enhancement of solubility and stability. Results from the ternary phase with CH and NS2 were superior to those using alone. Microwave treatment and high energised ball milling technique were used to alter the crystalline nature of OLM. All batches were designed and prepared by using a full 3 level 2 factorial design for studying effects on dependent variables. The improvement of wettability, solubility, dissolving rate, and stability is caused by the interaction of OLM with CH. In order to maximize this effect, NS2 was used as a surfactant. Results from FTIR, DSC, XRD, and NMR were used to confirm the compatibility and interaction studies. The surface morphology of the OLM and formulation were evident in SEM. An increase in solubility with the rate in the dissolution medium was observed by dissolution studies, saturation solubility studies, and drug content studies. Compared to OLM alone and formulations, solubility and stability were significantly improved by ball milling for optimized batch. Thus, one of the most efficient and novel ways to deal with the issue of BCS II drugs is through the use of microwave-assisted milling technology for enhancement of bioavailability.

ACKNOWLEDGEMENT

The authors would like to express their gratitude to CTX Life Sciences Limited and Lupin Research Park in Pune for providing free samples of a drug and a polymer for research work on crystal engineering. The principals of the Government College of Pharmacy in Karad and Gourishankar education society's Satara College of Pharmacy, Satara are also acknowledged by the authors for providing the necessary resources for the study and analysis. Regarding the provision of instrument facilities, the principal of the Late Dadasaheb Chavan Memorial Institute of Pharmacy in Masur is also acknowledged.

CONFLICT OF INTEREST

The authors declare that there is no conflict of interest.

ABBREVIATIONS

OLM: Olmesartan medoxomil; **BCS II:** Biopharmaceutical Classification System II; **AT 1:** Angiotensin 1; **AT 2:** Angiotensin 2; **FTIR:** Fourier Transform Infra-Red; **DSC:** Differential Scanning Calorimetry; **XRD:** X-ray Diffraction; **SEM:** Scanning electron Microscopy; **NMR:** Nuclear Magnetic Resonance; **RAS:** Rennin Angiotensin System; **ACE:** Angiotensin Converting Enzyme; **ATR:** Angiotensin receptor; **NS2:** Neusiline 2; **CH:** Chitosan; **UV:** Ultraviolet; **DMSO:** Dimethyl Sulphoxide; **MAGT:** Microwave assisted grinding technology; **ANOVA:** Analysis of varience; **% CDR:** Percentage Cumulative drug release.

SUMMARY

Microwave assisted grinding technology is a novel technique to tackle solubility issues of BCS II drugs. It can modify the crystalline state to metastable form. Current research work confirms the physical transformation of olmesartan medoxomil into highly soluble crystal particles. This can be analysed by using saturation solubility study, study of FTIR interaction, endothermic peak in DSC, crystallographic alteration in XRPD, surface morphology study by SEM, hydrogen bonding by NMR, dissolution study and stability study. This enhanced dissolution rate will minimise economical and biopharmaceutical burden of BCS II drugs.

REFERENCES

1. Mire DE, Silfani TN, Pugsley MK. A review of the structural and functional features of olmesartan medoxomil, an angiotensin receptor Blocker. J Cardiovasc Pharmacol. 2005;46(5):585-93. doi: 10.1097/01.fjc.0000180902.78230.fd, PMID 16220064.
2. Divya A, Ankita K, Rituparna RS, Praveen T, Gaurav G. Estimation of olmesartan medoxomil in tablet dosage forms using reverse phase high-performance liquid chromatography method. Eur J Biomed Pharm Sci. 2018;5(7):378-80.
3. Ishizuka T, Fujimori I, Kato M, Noji-Sakikawa C, Saito M, Yoshigae Y, *et al*. Human carboxymethylene butenolidase as a bioactivating hydrolase of olmesartan medoxomil in liver and intestine. J Biol Chem. 2010;285(16):11892-902. doi: 10.1074/jbc.M109.072629, PMID 20177059.
4. Majed AA, Bakheit AHH, *et al*. Olmesartan. Profiles Drug Subst Excipients Relat Methodol. 2017;42:241-86. doi: 10.1016/bs.podrm.2017.02.005.
5. B A, D N, Veerabrahma K. Development of olmesartan medoxomil lipid-based nanoparticles and nanosuspension: preparation, characterization and comparative pharmacokinetic evaluation. Artif Cells Nanomed Biotechnol. 2018;46(1):126-37. doi: 10.1080/21691401.2017.1299160, PMID 28290712.
6. Kumar O, Rani A, Saikishore V. Preparation and Charateization of olmesartan medoxomil solid dispersion for the development of orodispersable tablets. Indo-. Am J Pharmacol Sci. 2016;3(11):1330-6.
7. Gera S, Cheruvu S, Zakkula A, Sampathi S. Synthesis and evaluation of olmesartan medoxomil complex with SBE7 β-cd for enhanced dissolution and bioavailability. Int J Pharm Pharm Sci. 2016;8(1):333-43.
8. Chai R, Gao H, Ma Z, Guo M, Fu Q, Liu H, *et al*. *In vitro* and *in vivo* evaluation of olmesartan medoxomil microcrystals and nanocrystals: preparation, characterization, and pharmacokinetic comparison in beagle dogs. Curr Drug Deliv. 2019;16(6):500-10. doi: 10.2174/1567201816666190627143214, PMID 31244438.
9. Pandya NT, Jani P, Vanza J, Tandel H. Solid lipid nanoparticles as an efficient drug delivery system of olmesartan medoxomil for the treatment of hypertension. Colloids Surf B Biointerfaces. 2018;165:37-44. doi: 10.1016/j.colsurfb.2018.02.011, PMID 29453084.
10. Hannah ON, Mbah CJ. Study on the *in vitro* release kinetics of olmesartan-loaded optimized solid lipid nanoparticles. Int J Nanotechnol, (Rech). 2018;1(1):24-32.
11. Gajera A, Shah SK, Tyagi CK, Pandya S, Trivedi N. Formulation development of olmesartan medoxomil solid self microemulsifying drug delivery system. Indian J Appl Res. 2018;8(10):9-13.
12. Khattab WM, Zein El-Dein EE, El-Gizawy SA. Formulation of lyophilized oily-core poly-Ɛ-caprolactone nanocapsules to improve oral bioavailability of olmesartan medoxomil. Drug Dev Ind Pharm. 2020;46(5):795-805. doi: 10.1080/03639045.2020.1753763, PMID 32275456.
13. Zhang Q, Feng Z, Ren W, Zhao Y, Dushkin AV, Su W. Preparation of olmesartan medoxomil solid dispersion with sustained release performance by mechanochemical technology. Drug Deliv Transl Res. 2022;12(3):589-602. doi: 10.1007/s13346-021-00959-w, PMID 33860449.
14. Sahu R, Swain S, Mahapatra A, Negi RR, Samanta B, Nanda D, *et al*. Microwave-assisted high-energy ball milling synthesis of SBT nano-ceramics. Integr Ferroelectr. 2020;205(1):177-85. doi: 10.1080/10584587.2019.1675013.
15. Mishra RR, Sharma AK. Microwave-material interaction phenomena: heating mechanisms, challenges and opportunities in material processing. Compos A. 2016;81:78-97. doi: 10.1016/j.compositesa.2015.10.035.
16. Teufl D, Zaremba S. 2.45-GHz microwave processing and its influence on glass fiber reinforced plastics. Materials (Basel). 2018;11(5):838. doi: 10.3390/ma11050838, PMID 29783684.
17. Gavhane YN, Gurav AS, Yadav AV. Chitosan and its applications: a review of literature. Int. j. res. pharm. Int J Res Pharm Biosci. 2013;4(1):1-27.
18. Jadhav P, Pore Y. Physicochemical, thermodynamic and analytical studies on binary and ternary inclusion complexes of bosentan with hydroxypropyl-β-cyclodextrin. Bull Fac Pharm Cairo Univ. 2017;55(1):147-54. doi: 10.1016/j.bfopcu.2016.12.004.
19. Khattab WM, Zein El-Dein EE, El-Gizawy SA. Full factorial design and optimization of olmesartan medoxomil–loaded oily-core polymeric nanocapsules with improved *in vitro* stability. J Pharm Innov. 2021;16(4):673-87. doi: 10.1007/s12247-020-09479-5.
20. Garud AA, Shah RR. Formulation and optimization of liquisolid tablets of olmesartan medoxomil using 32 factorial designs. Int J Pharm Sci Res. 2017;8(11):4682-93. doi: 10.13040/IJPSR.0975-8232.8(11).4682-93.
21. Zhang Y, Wu Y, Qin Q, Wang F, Chen D. A study of the mechanism of microwave-assisted ball milling preparing ZnFe2O4. J Magn Magn Mater. 2016;409:6-9. doi: 10.1016/j.jmmm.2016.02.066.
22. Mulye SP, Jamadar SA, Karekar PS, Pore YV, Dhawale SC. Improvement in physicochemical properties of ezetimibe using a crystal engineering technique. Powder Technol. 2012;222:131-8. doi: 10.1016/j.powtec.2012.02.020.
23. Medarević D, Cvijić S, Dobričić V, Mitrić M, Djuriš J, Ibrić S. Assessing the potential of solid dispersions to improve dissolution rate and bioavailability of valsartan: *in vitro-in silico* approach. Eur J Pharm Sci. 2018;124:188-98. doi: 10.1016/j.ejps.2018.08.026, PMID 30144529.
24. Ahmad M, Gani A, Masoodi FA, Rizvi SH. Influence of ball milling on the production of starch nanoparticles and its effect on structural, thermal and functional properties. Int J Biol Macromol. 2020;151:85-91. doi: 10.1016/j.ijbiomac.2020.02.139, PMID 32068066.
25. Chashmniam S, Tafazzoli M. NMR investigation and theoretical calculations of the solvent effect on the conformation of valsartan. J Mol Struct. 2017;1148:73-80. doi: 10.1016/j.molstruc.2017.07.031.
26. Wood C, Alwati A, Halsey S, Gough T, Brown E, Kelly A, *et al*. Near infra-red spectroscopy as a multivariate process analytical tool for predicting pharmaceutical co-crystal concentration. J Pharm Biomed Anal. 2016;129:172-81. doi: 10.1016/j.jpba.2016.06.010, PMID 27429366.
27. Gurav AS, Sayyad FJ, Gavhane YN, Khakal NN. Development of olmesartan medoxomil-loaded chitosan microparticles: A potential strategy to improve physicochemical and micromeritic properties. Int J Pharm Pharm Sci. 2015;7(8):324-30.
28. Balakrishnaiah M, Gupta VRM, Nagar N. Enhancement of solubility and dissolution rate of olmesartan medoxomil by solvent evaporation technique. Pharm Lett. 2016;8(7):94-104.
29. Paarakh M, Jose PA, Setty CM, Christoper GV. Release kinetics – concepts and applications. Int J Pharm Res Tech. 2018;8(1):12-20.

Cite this article: Gurav AS, Kulkarni AS. Preparation and Optimization of Microwave-Assisted Ball-Milled Olmesartan Medoxomil with Chitosan Using Full 32 Factorial Design. Indian J of Pharmaceutical Education and Research. 2023;57(3s):s555-s563.